Phases and compounds composition analyze of ZnMgCa biodegradable alloy

IOP Conf. Series: Materials Science and Engineering **572** (2019) 012019 doi:10.1088/1757-899X/572/1/012019

Phases and compounds composition analyze of ZnMgCa biodegradable alloy

S (Dobriță) Popescu[1], S Stanciu[1], R Cimpoeșu[1*], B Istrate[2], I Știrbu[3], I Ioniță[1] and B A Prisecariu[4]
[1]Technical University "Gheorghe Asachi" from Iasi, Materials Science and Engineering Faculty, street Prof.dr.doc. D. Mangeron nr. 41, 700050, Iasi, Romania
[2]Technical University "Gheorghe Asachi" from Iasi, Mechanical Faculty, street Prof.dr.doc. D. Mangeron nr. 43, 700050, Iasi, Romania
[3]Technical University "Gheorghe Asachi" from Iasi, street Prof.dr.doc. D. Mangeron number 43, 700050, Iasi, Romania
[4]"Grigore T. Popa" University of Medicine and Pharmacy, Universitatii Street, number 16, 700115 Iasi, Romania

E-mail: ramona.cimpoesu@tuiasi.ro

Abstract. Besides biocompatible materials, a new class of metallic materials with medical applications dedicated to specific traumas is that of biodegradable materials. Zinc-based materials are mentioned as the 'Calcium of the XXI century'. Zn has been considered as one of the newest promising biodegradable metallic metals together with Mg-based and Fe-based alloys. A new experimental composition of ZnMgCa alloy was obtained using an induction furnace from high purity zinc, magnesium and calcium materials. The material chemical compounds and phases were determined using EDS Bruker detector and XRD X'Pert equipment in molded state of the alloy. Microstructure of the alloy was determined using scanning electron microscopy and the distribution of constituents using VegaTescan software.

1. Introduction

In last year's, Zinc based alloys present a great interest for researchers as biodegradable materials. Alloys with Zn base present a good biocompatibility and a perfect corrosion rate for many medical applications [1-3]. In order to control the behavior of an alloy for implants many processing techniques like melting, deformation, laser treatment or synthesis [4] have been applied. Besides Mg-base and Fe-base alloys used as biodegradable systems this new class of materials present a corrosion rate between first two and proper mechanical characteristics. In case of zinc alloys, a zinc phase is most common structural component formed during the solidification stage with a crucial role in degradation behavior of the material. Its evolution behavior has a crucial role in final structure of the alloy directly connected to the final properties of the material including corrosion resistance [5]. Based on these arguments it is of scientific interest to analyze in order to control the solidification of Zinc base alloys.

In a general way the idea of degradable biomaterials is simple as the name, some implants only temporarily require their presence on injured bone to support the healing process of diseased tissue. This temporary intervention (implant) is only considered in certain cases such as cardiovascular, orthopedic and pediatric. Ideally, biodegradable coronary stents should provide a compromise between

mechanical integrity and degradation rate [6, 7]. Degradation should begin at a very low rate to maintain the optimal mechanical integrity of the stent until the process of complete remodeling takes place completely, a process lasting from 6 to 12 months, and then with the progress of degradation, the mechanical properties will be lost. After the recovery operation is completed, the degradation rate must be sufficiently high so that no intolerable accumulations of degradation material or debris occur around the implementation area or the main organs. Biodegradable metals must provide adequate mechanical support to support the healing process during implantation. However, it is difficult to define a support period as close as possible to medical reality depending on the various interventions that take place [8, 9].

In this article the authors present the analyze of phases and compounds of a new experimental alloy based on Zinc that can be used as biodegradable material in medical applications.

2. Materials and methods

An experimental alloy ZnMgCa based was obtained using induction furnace with Ar from high purity zinc (99,99%) and MgCa master alloy. Phases were determined by X-ray diffraction (XRD) using X-Pert equipment. The microstructure was analyzed after etching by FeCl3 using scanning electron microscopy (SEM VegaTescan LMHII equipment with SE detector for 30 kV filament heating). Chemical composition at macro and micro scale were realized using energy dispersive X-ray analysis (EDS) technique by EDAX Bruker detector for automatic and element list modes. Point analyze (focused primary electrons beam on 90 nm spot) was used to determine the different compounds of the alloy that appear in the alloy. Line mode (variation of main elements Zn, Mg and Ca) analyze was used to highlight the differences between the matrix and the eutectic compounds of the alloy.

The distribution of Zn, Mg and Ca elements were highlighted by Mapping mode analyze. The experimental alloy Zn8.5Mg1.5Ca has a phase composition: 53% (Zn+ eutectic Mg2Zn11)+47%MgZn2 (approximate volume fraction of each phase was obtained by image analysis) [10]. The experiments were performed in accordance with the occupational health and safety laws and regulations in order to eliminate all the risks and dangers which can affect the human resource during the experiment procedures [11-14].

3. Results and discussions

In Figure 1 the XRD phase diagram of ZnMgCa alloy is presented with the identification of 33 representative peaks for different phases (table 1). In order to establish a degradation behavior of experimental alloy ZnMgCa we firstly do an investigation of the material components and after that in a further work the authors will establish each phase behavior in an electrolyte solution.

From Figure 1, XRD phase diagram of ZnMgCa alloy, we manage to identify next phases (indeces): simonkoleite: 1 (011), 2(012); zinc: 3(010), 6(121), 10 (004), 13(221), 19(027), 20(1-11), 32(150), 33(244); Zn_2Mg: 4(110), 5(013), 21(20-5), 26(237), 28(212), 31(020); ZnMg: 6(121), 11(13-5), 12(12-2), 15(026), 17(222), 18(223); ZnO: 7(10-3); $Zn_{11}Mg_2$:8(11-3), 16(222), 24(354); Ca_7Mg: 12b(102); Zn_2Ca: 23(353), 29(442); Zn_3Ca: 27(212). The dimensional characteristics of the identified phases are presented in table 1. The values are retrieved from Crystallography Open Database [15-20]. The alloy present two oxides after the oxidation of zinc in air (simonkoleite and ZnO) compounds that naturally appear at permanent contact of the alloy with air.

The experimental alloy ZnMgCa present 3 different crystal systems (table 1) with different cell characteristics that will present different properties by corrosion behavior point of view or mechanical properties. The behavior of the entire sample depends now on how these phases influence the general properties of the alloy.

In Figure 2 SEM images of ZnMgCa microstructure are presented at 1500x amplification power and in b) with 3 points selected for chemical composition analyze. The alloy Zn8.5Mg1.5Ca contain $MgZn_2$ platonic solids shape compounds with uneven boundaries based on the peritectic reaction $L+MgZn_2 = Mg_2Zn_{11}$. The space between the platonic solids was filled with $Zn+Mg_2Zn_{11}$ eutectic [21]. As shown in Figure 2 a high number of dendritic primary Zn-rich crystals are distributed in the

dark-grey eutectic matrix throughout the whole specimen (the black hole from the left top of the specimen, Figure 2 b), is a shrinkage cavity). The dendritic primary crystals have a random alignment and orientation. Apparently the dendrites present different formation shapes like columnar dendritic, snow-flake, thin plates, cross-like and globular elements, Figure 2 a) and b) [22, 23].

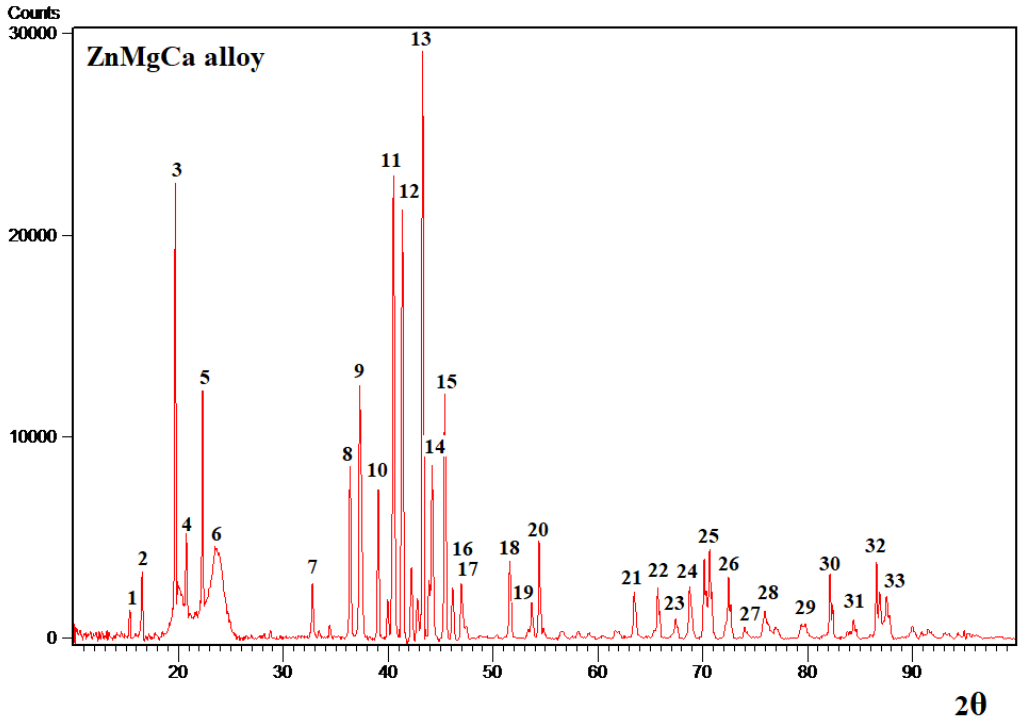

Figure 1. XRD phase diagram of ZnMgCa alloy.

Table 1. Phase components characteristics identified in experimental ZnMgCa alloy.

Phase/characteristics	Crystal system:	a (Å)	b (Å)	c (Å)	Volume of cell (10^6 pm^3):	Calculated density (g/cm^3)
Zn	Hexagonal	2,6645	2,6645	4,9453	30,41	-
Zn_2Mg	Hexagonal	5,2225	5,2225	8,5684	202,39	5,09
Zn_3Mg_7	Cubic	14,170	14,170	14,170	2845,18	-
$Zn_{11}Mg_2$	Cubic	8,552	8,552	8,552	625,47	-
Zn_3Ca	Hexagonal	9,168	9,168	7,327	533,34	-
Zn_2Ca	Orthorhombic	4,591	7,337	7,667	258,26	-
ZnO	Hexagonal	3,289	3,289	5,307	49,719	5,44
Simonkoleite ($Zn_5(OH)_8Cl_2.H_2O$)						

Table 2 presents the chemical composition of ZnMgCa experimental alloy determined by EDS detector in three characteristic points, Figure 2 b). Chemical composition determinations were made using two different modes: automatic and element list. All phases present an atmospheric oxidation proven by the presence of oxygen on the surface. The dendritic arms present a higher oxidation compare with the matrix but with a reduce percentage (less than 1% wt). Calcium element doesn't form dendrites being assimilated by zinc in the matrix in order to form Zn_2Ca and Zn_3Ca compounds. The presence of carbon on the alloy is put on contamination of the material from atmosphere or from the graphite crucible used in melting/pouring stages of elaboration process [24-26]. By elemental

chemical composition part zinc element, normally considering the high percentage, present the biggest oxidation process [26-28]. Using element list mode, we establish the chemical composition of the three different formations identified by SEM images without the influence of oxygen. The first type of dendrite (point 2) are almost calcium free and based on zinc and magnesium. The second dendrite type (point 3) present a calcium percentage but can be taken from the material matrix because the point 3 present a mixed area of matrix and dendrites so further research must be made in order to establish the final values of chemical composition for the main components of the alloy.

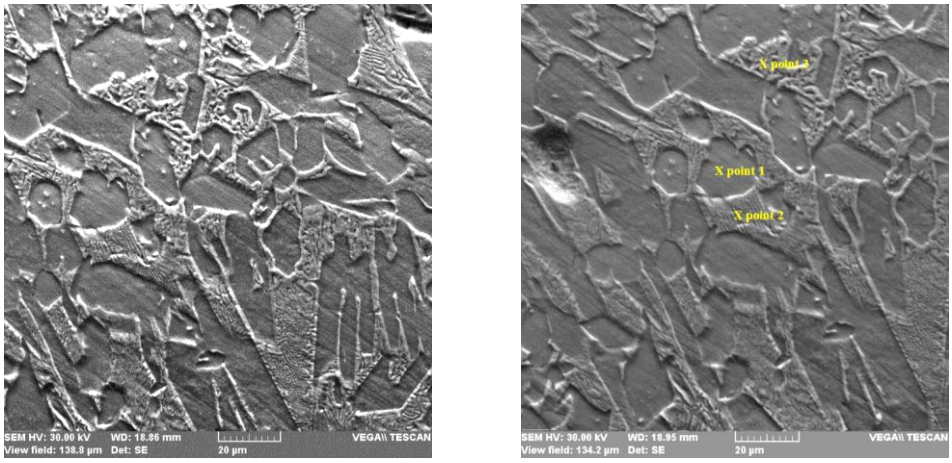

a) b)

Figure 2. SEM Images of ZnMgCa microstructure a) 1500x and b) 1500x with 3 points selected for chemical composition analyze.

Table 2. Chemical composition (wt and at%) of ZnMgCa experimental alloy.

Element/area		**Zinc**		**Magnesium**		**Calcium**		**Oxygen**		**Carbon**	
		wt%	at%	wt%	at%	wt%	at%	wt%	at%	wt%	at%
Alloy (~)	Element list	90		8.5		1.5		-	-	-	-
	Automatic	67.51	34.85	8.1	11.24	1.02	0.86	18.05	38.09	5.32	14.96
Point1	Element list	93.04	86.27	3.70	5.60	3.26	8.13	-	-	-	-
	Automatic	69.84	35.75	4.03	5.55	0.21	0.18	19.71	41.22	6.21	17.31
Point2	Element list	93.47	84.4	6.23	15.14	0.3	0.44	-	-	-	-
	Automatic	69.15	36.7	2.17	3.1	4.35	3.77	19.3	41.87	5.04	14.56
Point3	Element list	91.15	83.83	5.87	8.81	2.98	7.37	-	-	-	-
EDS error %		1.2		0.5		0.1		1.5		0.7	

Evaluation of chemical homogeneity of the alloy was further made using Line, Figure 3, and mapping, Figure 4, analyze modes. Figure 3 present the elements distribution using the Line analyze mode on the line made on microstructure (down part of the image) a) Zn, Mg and Ca and b) detail of Mg and Ca variation.

Zinc element, clearly, present a reduce variation of chemical composition with percentages between 78-100%, based on the compounds formed in the alloy, Figure 3 a). Calcium presence is confirmed on matrix of the material and the magnesium participation in dendrites formation also, Figure 3 b). Their variation is based on the participation in formation of dendrites or the spread in the metallic matrix. Distribution of the elements, Figure 4 b) and c), present a wide spread of zinc on the

majority areas of the alloy with small black exceptions that represent $MgCa_7$ phases or magnesium oxides.

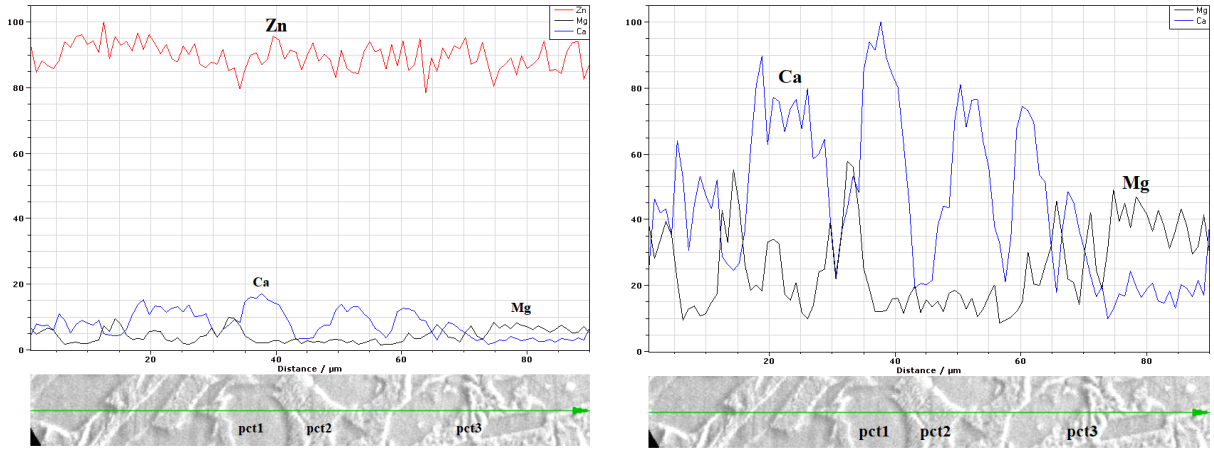

a) b)

Figure 3. Elements distribution on selected line, down part of the image for a) Zn, Mg and Ca and b) detail of Mg and Ca variation.

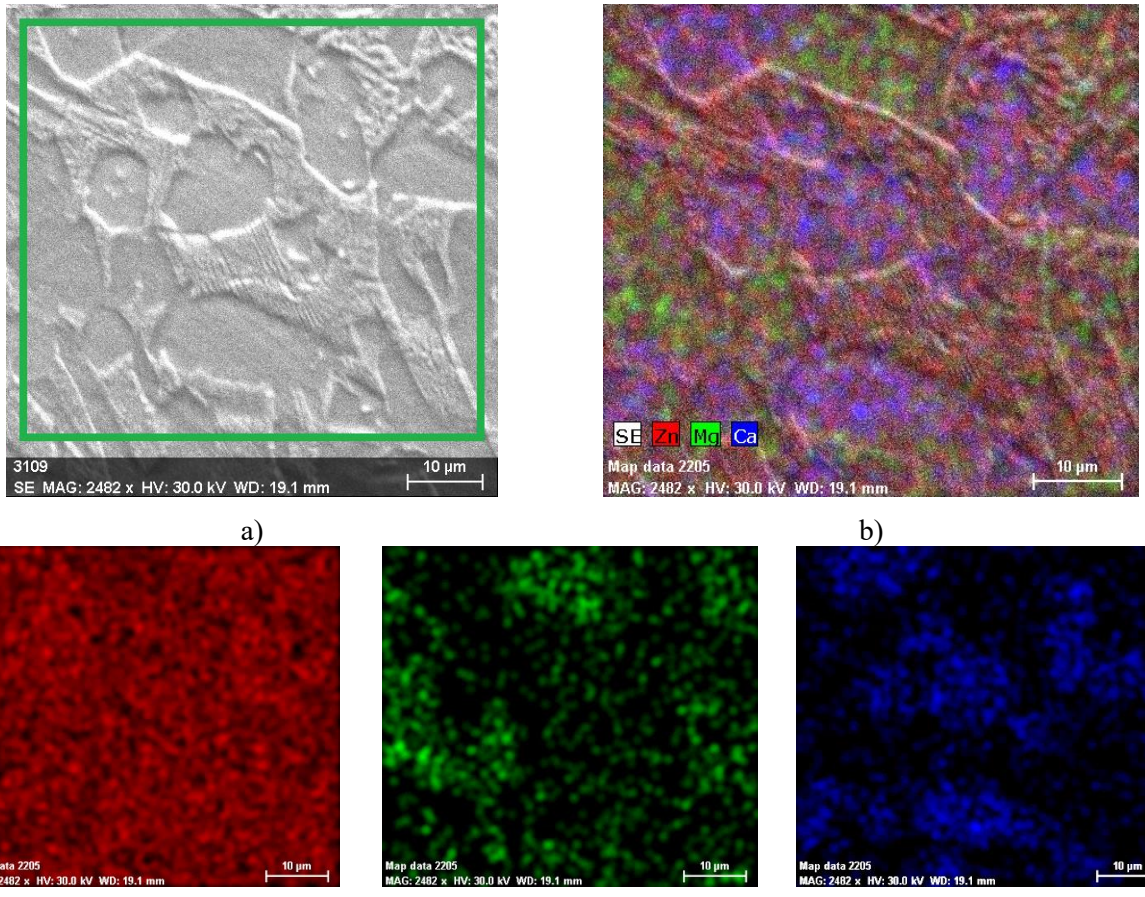

a) b)

c) d) e)

Figure 4. Distribution of Zn, Mg and Ca elements in Zn8.5Mg1.5Ca alloy a) surface selected for analyze, b) distribution of all elements, c) Zn distribution, d) Mg distribution and e) Ca distribution.

Magnesium and calcium distributions place these elements especially on matrix and less on dendrites, even if the presence of magnesium was already established. Calcium is observed on spaces between the zinc based dendrites. The distribution of calcium and magnesium in the alloy is important for further behavior of the material in electrolytic solution. The good spread of Ca compounds on the material represent an advantages for a homogeny general degradation of the alloy.

4. Conclusions

A new experimental alloy based on zinc was obtain in an induction furnace that can be proposed for medical applications as biodegradable element. Beside zinc as pure state other seven phases were identified using XRD, SEM and EDS techniques. Phase are based on zinc combination with magnesium and calcium elements (Zn, Zn2Mg, Zn3Mg7, Zn11Mg2, Zn3Ca and Zn2Ca) and some zinc oxides on the surfaces from contact with atmospheric environment and chemical reactant FeCl3 (ZnO and Simonkoleite - (Zn5(OH)8Cl2.H2O)). Calcium element was identified especially on matrix material and less on dendrites. Dendrites formed (zinc and magnesium) present a higher oxidation compared with matrix material. Distribution of zinc is homogeneous on the entire alloy and calcium and magnesium present areas also uniformly spread. The chemical composition homogeneity is an important aspect in order to obtain a generalized corrosion of the material. Magnesium compounds present a higher oxidation in dendrite participation and less in matrix where the stability to oxygen is much better.

5. References

[1] Su Y, Cockerill I, Wang Y, Qin Y X, Chang L, Zheng Y and Zhu D 2019 *Trends in Biotechnology* **37(4)** 428-441
[2] Venezuela J and Dargusch M S 2019 *Acta Biomaterialia* **87** 1–40
[3] Prosek T, Nazarov A, Bexell U, Thierry D, Serak J, 2008 *Corrosion Science*, **50** 2216–2231
[4] Li L, Zhang R, Ban C, Zhang H, Liu T, Zhang H, Wang X, Esling C and Cui J 2019 *Materials Characterization* **151** 191-202
[5] Vojtěch D, Kubásek J, Šerák J and Novák P 2011 *Acta Biomaterialia* **7** 3515–3522
[6] Rățoi M, Stanciu S, Cimpoeșu N, Cimpoeșu I, Constantin B and Paraschiv C 2013 *Advanced Materials Research* **814** 110-114
[7] Cimpoeșu N, Trincă L C, Dascălu G, Stanciu S, Gurlui S O and Mareci D 2016 *Journal of Chemistry* 9520972
[8] Maria W, Wiktor B, Jakub K and Piotr B 2018 *Materials Characterization* **142** 187–194
[9] Dumitru M and Cimpoesu N 2010 *Metalurgia Internaţional XV* 35-41
[10] Wen P, Jauer L, Voshage M, Chen Y, Poprawe R and Schleifenbaum J H 2018 *J. Mater. Process. Technol.* **258** 128–137
[11] Bejinariu C, Darabont D C, Baciu E R, Georgescu I S, Bernevig-Sava M A and Baciu C 2017 *Sustainability* **9** 1263
[12] Bejinariu C, Darabont D C, Baciu E R, Ionita I, Sava M A B and Baciu C 2017 *Environmental Engineering and Management Journal* **16** 1395–1400
[13] Darabont D C, Moraru R I, Antonov A E and Bejinariu C 2017 *Qual Access Success* **18** 11–14
[14] Darabont D C, Antonov A E, Bejinariu C 2017 *In 8th International Conference on Manufacturing Science and Education (MSE 2017) - Trends in New Industrial Revolution*, Bondrea I, Simion C, Inta M (Eds) E D P Sciences: Cedex A, 2017 **121** 11007
[15] http://www crystallography net/cod/
[16] Mureșan E I, Puitel A, Pui A, Radu C D, Tampu D, Cimpoesu N and Sandu I 2016 *Revista de Chimie* **67(4)**
[17] Dobrita S, Istrate B, Cimpoesu N, Stanciu S, Apostol V, Cimpoesu R, Ionita I and Paraschiv P 2018 *Book Series: IOP Conference Series-Materials Science and Engineering* **374** 012027
[18] Cimpoeșu N, Săndulache F, Istrate B, Cimpoeșu R and Zegan G 2018 *Metals* **8(7)** 541
[19] Yue R, Huang H, Ke G Z, Zhang H, Pei J, Xue G H and Yuan G Y 2017 *Materials*

Characterization **134** 114–122
[20] Prosek T, Nazarov A, Bexell U, Thierry D and Serak J 2008 *Corrosion Science* **50** 2216–2231
[21] Yao C Z, Wang Z C, Tay S L, Zhu T P and Gao W 2014 *J. Alloy. Compd.* **602** 101–107
[22] Cerempei A, Muresan E I¸ Cimpoesu N, Carp-Carare C and Rimbu C, 2016 *Industrial Crops and Products* **94** 216–225
[23] Dumitru M and Bujoreanu L G 2002 *Revista de metalurgie* **38** 464-468
[24] Baltatu M S, Vizureanu P, Cimpoesu R, Abdullah M M A and Sandu A V 2016 *Revista de Chimie* **67** 2100-2102
[25] Nejneru C, Perju M C, Sandu A V, Axinte M, Quaranta M, Sandu I, Costea M and Abdullah M M A 2016 *Revista de chimie* **67(6)** 1191-94
[26] Barbinta AC, Mareci D, Chelariu R, Bolat G, Munteanu C and Cho K *2014 Materials and Corrosion-Werkstoffe und Korrosion* **65(10)** 1017-1023
[27] Istrate B, Mareci D, Munteanu C, Stanciu S, Luca D, Crimu C I and Kamel E 2015 *Journal of Optoelectronics and Advanced Materials* **17(7-8)** 1186-1192
[28] Tarnita D, Tarnita DN, Bizdoaca N, Tarnita C, Berceanu C and Boborelu C 2009 *Romanian Journal of Morphology and embryology* **50** 447-452

Acknowledgments
Part of this work was supported by a grant of Romanian Ministery of Research and Innovation, CCCDI –UEFISCDI, project number PN-III-P1-1.2-PCCDI-2017-0239, within PNCDI III, ORTOMAG.